



Article

How Cool Are Allotment Gardens? A Case Study of Nocturnal Air Temperature Differences in Berlin, Germany

Annemarie Tabea Rost ^{*}, Victoria Liste, Corinna Seidel, Lea Matscheroth, Marco Otto ^{*} , Fred Meier and Daniel Fenner 

Chair of Climatology, Institute of Ecology, Technische Universität Berlin, Rothenburgstraße 12, D-12165 Berlin, Germany; v.liste@hotmail.com (V.L.); corinna.e.seidel@campus.tu-berlin.de (C.S.);

l.matscheroth@campus.tu-berlin.de (L.M.); fred.meier@tu-berlin.de (F.M.); daniel.fenner@tu-berlin.de (D.F.)

^{*} Correspondence: annemarierost@gmail.com (A.T.R.); marco.otto@klima.tu-berlin.de (M.O.)

Received: 31 March 2020; Accepted: 8 May 2020; Published: 13 May 2020



Abstract: Urban green infrastructures have been extensively studied for their ability to mitigate the urban heat island (UHI) effect. However, allotment gardens (AGs)—a prominent type of urban green infrastructure within many European cities—have not yet been comprehensively investigated concerning their microclimates. In this study, nocturnal air temperatures (T_N) in 13 AG complexes (AGCs) were measured during the summer of 2018 in Berlin, Germany. These were compared to measurements in densely built-up urban areas (URB), two large inner-city parks and rural areas (RUR). On average, the assessed AGCs were 2.7 K cooler at night than URB. Most of the investigated AGCs (11/13) displayed a larger mean T_N difference to URB ($\overline{\Delta T_{N\ AGC}}$) than the examined urban parks. RUR showed the largest differences to URB ($\overline{\Delta T_{N\ RUR}}$), indicating a UHI effect. Furthermore, the influence of land surface characteristics of the AGCs on $\overline{\Delta T_{N\ AGC}}$ was analyzed. $\overline{\Delta T_{N\ AGC}}$ decreased significantly as the floor space index around AGCs increased. The analysis of the shape complexity also produced a significant positive correlation with $\overline{\Delta T_{N\ AGC}}$. In contrast, size and distance to the city center of an AGC decreased significantly with increasing $\overline{\Delta T_{N\ AGC}}$. This study provides first insights into the microclimate of AGs and influencing variables concerning T_N .

Keywords: allotment gardens; community gardens; urban green infrastructure; urban climate; microclimate; air temperature; Berlin; urban heat island

1. Introduction

The distinctive features of urban areas [1] result in an altered energy exchange compared to their rural surroundings. Urban areas are characterized by a lower albedo, higher thermal conductivity and higher heat capacities of building materials [2]. Further, they show reduced convective cooling, as well as lower evapotranspiration rates [2]. This leads to the well-studied phenomenon of the urban heat island (UHI) with generally higher air temperatures (T) in urban areas in comparison to the surrounding rural areas [2,3].

UHI intensity, defined as the difference in T between the city and the surrounding rural area, varies in time and space. It is influenced by seasons, time of day, meteorological, geographical and physical properties. This includes land use patterns, such as local climate zones (LCZs) [1,4–6]. The UHI effect is especially prominent during nights with calm and clear weather conditions [7,8]. Under these conditions, the energy budget of the canopy layer can be simplified to be primarily determined by the outgoing longwave radiation [7,8]. The loss of longwave radiation from storage is strongly influenced by the sky view factor (SVF) and properties of the urban materials and vegetation [8–10]. Typically, large green spaces are found to mitigate the UHI effect at night [11].

The properties of urban green infrastructure, especially urban parks were widely studied in recent years [12,13]. Lower T in parks compared to surrounding built-up areas are caused by a range of factors during the day, including evapotranspiration and shading of incoming solar radiation [14,15]. The permeable surfaces of parks have the ability to retain water for evapotranspiration, as well as to absorb and store heat [16]. The aforementioned T difference is referred to as park cool island (PCI) [16]. PCIs within a city can help to mitigate the negative effects of UHI on human wellbeing and health [9,16]. The nocturnal PCI effect is particularly beneficial for human sleep, by improving the thermal conditions in surrounding areas of the park.

During day- and night-time land surface characteristics, e.g., park type, shape, size and surrounding land use influence the PCI [5,15,17]. The cooling capacities of parks at night differ, e.g., in relation to the density and distribution of trees [18,19]. Spronken-Smith and Oke [19] stated that conditions that favor PCI during the day, such as tree shade and soil moisture, could delay the PCI effect at night. Therefore, open parks cool down faster than forested parks during night-time. Here, the outgoing longwave radiation, a lower heat storage and the conduction of vegetative areas compared to the surrounding urban fabric play an important role [19]. The nocturnal cooling potential can also be affected by the evapotranspiration around sunset [19].

Previous studies have shown that urban parks with a lower edge-to-area ratio are cooler than those with a high ratio (i.e., increased complexity of shape) [20–22], due to less contact with the surrounding urban area [23,24]. Larger parks have also been found to be cooler than smaller ones [14,25]. However, the correlation of park size and T was found to be non-linear [16,21]. Lin et al. [26] and Egerer et al. [27] found that urban gardens with a less densely built-up vicinity are cooler than those with a high ratio of built-up structures in their surroundings. Research about small-scale atmospheric processes of urban green infrastructure provides valuable insights, especially for landscape and urban planning, as well as for adaptation to climate change [28,29]. To complement previous work, investigations similar to those for urban parks or urban gardens could be applied to further types of urban green infrastructure, such as allotment gardens (AGs).

AGs account for 13% of urban green infrastructure in Berlin, Germany [9]. In central and northern Europe, the number of AGs has risen since the industrialization at the beginning of the 18th century [30]. The number and size of AGs continues to rise in southern Europe (e.g., Spain, Portugal and Greece), especially since the financial recession during the 2000s [31]. However, the number of AGs is steadily declining in central Europe because of real estate pressure [32]. In Berlin, for example, both, the number and total size of AGs decreased by 4% between 2012 and 2018 [33,34]. Figure 1 shows an example of a single garden plot within an AG in Berlin.

In Germany, AGs originate from the “Armengärten” (gardens for the poor) at the beginning of the 19th century. Agricultural fields were divided into smaller plots in order to provide the poor population with areas for agricultural subsistence. A second root goes back to the orthopedist Schreber (1808–1861). He called for places where the ailing children of factory workers could play in the fresh air. After his death, the idea was put into practice with the creation of playgrounds surrounded by gardens, which later became AGs. In Berlin, the development of AGs was directly linked to the social problems of the growing industrial metropolis at the end of the 19th century. Unlike urban parks, the purpose of AGs was and still is the provision of food. Today, however, they are increasingly used for recreational purposes [34]. Social cohesion, local community building [35] and physical activity for the gardeners are other cultural ecosystem services (ESs) provided by AGs. Recent studies focus on additional ESs of AGs, such as the improvement of soil quality [31], water retention and prevention of erosion [36].

Therefore, AGs represent an important part of urban green infrastructure [37] and show differences to urban parks. They feature a greater diversity of plants, e.g., a higher percentage of annual vegetation and flowering shrubs and trees [38]. Further, they display more complex shapes and specific structures, such as vegetable beds and small garden sheds [39], leading to varying degrees of sealed soil. AGs provide habitats for plants and animals, thereby contributing widely to urban biodiversity [40]. The federal allotment garden law [41] stipulates the characteristics of AGs, e.g., tall trees are prohibited

and one third of each garden plot must be covered by edible plants. Most AGs are located in complexes of several individual garden plots (e.g., as in Figure 1) along with communal facilities [41]. Typically, AGs are frequently irrigated. This could lead to increased cooling properties [26] since irrigated vegetation has lower surface temperatures than water-stressed vegetation [42]. Due to these characteristics, AGs may provide climate regulating ESs for the city similar to urban parks. However, there are far fewer studies regarding microclimatic properties and cooling potential of AGs compared to those of urban parks [31,32,43]. For example, Egerer et al. [27] focus on the influence of T on watering behavior of AG tenants. In another study by Schlegelmilch [43], the cooling potential of one AG on its surroundings was investigated. To date, these are the only studies focusing on the microclimate of AGs to the authors' knowledge.



Figure 1. Example of a plot (a) within an allotment garden complex (AGC6) (b) in Berlin (52.483948 N/13.329340 E). Source: Photo of plot (a) taken by authors; aerial view (b): ©2020 GeoBasis-DE/BKG, GeoContent, Maxar Technologies.

The intention of the present study is, to provide first insights into the microclimatic properties of AGs compared to surrounding built-up and rural areas at night. Previous research has demonstrated that the highest cooling effects of urban green infrastructure occur during night-time [19]. To address this, observational data of near-surface T was collected during the study's measurement campaign -in summer 2018-across multiple AGs throughout the urban area of Berlin. In particular, we address the following research questions:

1. How does the mean nocturnal T of AGs differ from densely built-up areas (URB), urban parks and rural areas (RUR) in the study area?
2. How and to what extent, do mean T differences between URB and AGs correlate with micro-scale land surface characteristics of AGs?

2. Materials and Methods

2.1. Study Area

Berlin, the capital and largest city of Germany by both area (891.1 km²) and population (3,723,914 inhabitants) [44] is characterized by a maritime temperate climate (sub-zone Cfb), according to the Köppen climate classification [45,46]. Berlin's area is distinguished by vegetated areas (39%, including AGs), built-up areas (35%), areas for infrastructure and transport (20%) and water bodies (6%) [47]. AGs make up around 5% of the area of Berlin [9], covering 29.0 km² and comprising 71,473

garden plots as of May 2018 [33]. The size of AGs in Berlin ranges from 0.0002 km² to 1.1 km² [48]. An AG complex is defined as a combination of multiple individual gardens with communal facilities such as playgrounds, clubhouses and paths [41].

2.2. Selection of Measurement Sites and Land Surface Characteristics of AGs and Surroundings

In this study, we define one AG complex (AGC) as a spatially coherent entity of several garden plots. All AGCs that are less than 20 m apart from each other are considered as one AGC for the purpose of this study. We set a limit of 20 m to avoid the influence of traffic passing through the space, based on the mean street width of Berlin, which is approximately 20 m [49]. This produced a total number of 555 AGCs in the city of Berlin.

The land surface characteristics of size, distance to the city center (here, Alexanderplatz [9]), perimeter and edge-to-area ratio of each AGC were calculated. Additionally, the floor space index [50] and sealing [51] within AGCs and around them in a buffer of 500 m were determined. Table 1 gives an overview about all used land surface characteristics and their abbreviations. It also shows the mean values for all AGCs in Berlin and for those sampled during the measurement campaign. Detailed distributions of all AGCs in Berlin and the sampled AGCs for each land surface characteristic can be found in Appendix A. Compared to all AGCs in Berlin, the sampled AGCs are on average closer to the city center, larger in size, with lower shape complexity and more building development around them (Table 1).

Table 1. Used land surface characteristics, their abbreviations, descriptions, units and the comparison between all allotment garden complexes (AGCs,555) and sampled AGCs (13) in Berlin. Depicted are the mean values for each characteristic by each group. AGC: FSI: Floor space index; ALEX: Measurement station ‘Alexanderplatz’.

Land Surface Characteristic	Abbreviation in this Study	Description	Unit	Sampled AGCs	All AGCs
Floor space index within AGCs	FSI inside	total covered area on all floors of all buildings on a certain plot divided by the area of the plot; within the borders of an AGC	–	0.3	0.4
Floor space index within a buffer of 500 m around AGCs	FSI outside	total covered area on all floors of all buildings on a certain plot divided by the area of the plot; in a 500-m buffer around an AGC	–	1.0	0.3
Degree of sealed surface within AGCs	Sealing inside	Degree of impervious surfaces (including buildings) of the total surface area; within the borders of an AGC	%	30.6	33.3
Degree of sealed surface within a buffer of 500 m around AGCs	Sealing outside	Degree of impervious surfaces (including buildings) of the total surface area; in a 500 m buffer around an AGC	%	49.0	35.4
Size	Size	Size of an AGC	km ²	0.1	0.05
Perimeter	Perimeter	Perimeter of an AGC	km	2.5	1.45
Edge-to-area ratio	Shape complexity	Perimeter divided by the area	km ⁻¹	40.6	67.8
Distance to ALEX	Distance to city center	Distance from the border of an AGC to the measurement station ALEX	km	7.1	10.8

2.3. Measurement Campaign

The measurement campaign was conducted from 31 July to 3 October 2018. A total of 39 measurement sites in 15 AGCs were sampled in close collaboration with the owners of the garden plots. The sampled AGCs were chosen based on their proximity to the geographical city center ALEX. Further, the aim was to analyze a variety of AGCs with different sizes, shape complexities and degrees of built-up area surrounding it. When selecting the measurement sites within the AGCs, the aim was to sample at different locations within each AGC (at least one nearer to the edge and one in

the center). However, the final choice was limited by the willingness of the garden owners to cooperate. At each of the 39 measurement sites, T was measured by an Easy Log EL-USB-2 (resolution of 0.5 °C, specific device error of 0.5 K between 0–30 °C) at 10-min intervals (instantaneous values). Each logger was placed inside a radiation screen (white plastic, passive ventilation), tied to a metal pole 1.70 m above ground level and placed facing north. The SVF was calculated for each site from a fish-eye photo (taken at a height of 1.20 m in July with full foliage) using the software SOLWEIG 2015a 1D [52]. In order to make the measurement sites comparable, we only selected sites within garden plots with a SVF higher than 0.59. Throughout the measurement campaign, each logger was checked to ensure its proper functionality and to save the data. The raw data from the measurement sites is provided online [53].

To compare T from AGCs with other urban areas within Berlin and rural areas outside the city, seven additional measurement stations were selected, based on their LCZ [6]. The measurement stations for urban parks were Tiergarten as ‘Park1’ (2.1 km², partly irrigated, dense trees; LCZ A) and the former airport Tempelhofer Feld as ‘Park2’ (3.0 km², not irrigated, low plants; LCZ D). Park1 and Park2 were selected based on the availability of data and to cover different park types [4]. Both are the largest inner-city parks in Berlin. To characterize T of densely built-up areas in Berlin, three measurement stations were chosen: Alexanderplatz ‘ALEX’, Bamberger Straße ‘BAMB’ and Dessauer Straße ‘DESS’ (all compact midrise; LCZ 2, as in [4]). T data at these three stations was averaged to one synthetic time series referred to as ‘URB’. Rural areas are represented in this study by the stations Kaniswall ‘KANI’ and Dahlemer Feld ‘DAHF’ (both scattered trees; LCZ B). T data at these two sites was also averaged into a synthetic time series, ‘RUR’, as in Fenner et al. [54]. The seven stations are maintained by the German Weather Service (DWD CDC [55]) and the Technische Universität Berlin as part of the Urban Climate Observation Network (UCON, [56]). Figure 2 provides an overview of the locations of all AGCs, the measurement stations and the FSI of Berlin. A detailed description of all AGCs and measurement stations can be found in Appendix B.

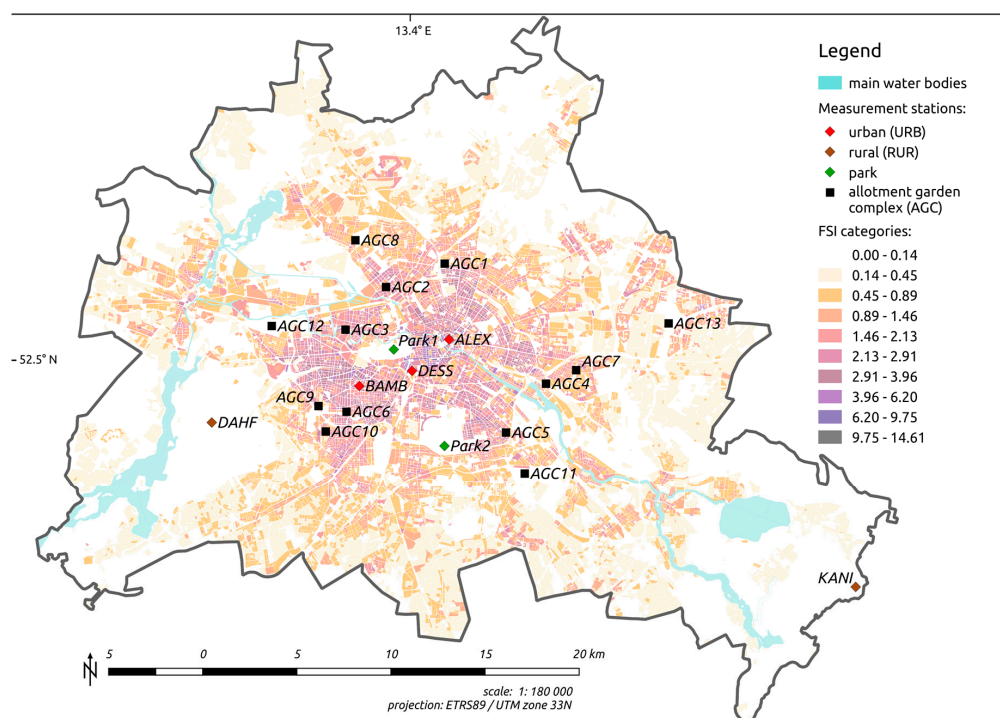


Figure 2. Map of Berlin displaying the positions of allotment garden complexes (AGCs) and measurement stations as well as floor space index (FSI). The gray line indicates the administrative border of Berlin.

2.4. Data Preparation

Comparison measurements were conducted after the measurement campaign to evaluate the accuracy of the measurement devices (climate chamber experiment with temperature range: 0–30 °C, seven temperature levels at 5 K steps). The test showed that the devices were precise, relatively to their accuracy of 0.5 K. However, the exclusion of erroneous data series (see Appendix C) led to a final sample size of 35 measurement sites in 13 AGCs. This resulted in at least two measurement sites in each AGC. The AGCs were numbered consecutively according to their distance to the city center (Table 2).

Table 2. Classification of the sampled allotment garden complexes (AGCs) according to their distance to the city center.

Distance (km)	4.1–5	5.1–6	6.1–7	7.1–8	8.1–9	>9
AGC	1 & 2	3, 4 & 5	6 & 7	8 & 9	10 & 11	12 & 13

For the following analysis, night-time values from 0:00 a.m. (UTC + 1; several hours after sunset), to 4:00 a.m. (UTC + 1; before sunrise) were chosen. During these hours, micro- to local-scale T differences are pronounced in Berlin [4,54,56,57]. Further, calm and clear weather conditions facilitate the formation of typical local climate phenomena such as the UHI [6–8,58]. The measurement period was therefore stratified according to the following conditions, analogue to Quanz et al. [59]: mean cloud cover ≤ 3 octas, mean wind speed ≤ 3 m/s and no precipitation during the night-time interval and no precipitation during the previous day. The application of these thresholds resulted in six remaining nights (04/08; 07/08; 17/08; 20/08; 23/08; 30/09). Atmospheric conditions across the whole measurement period and the nights with calm and clear weather conditions are shown in Table 3.

Table 3. Mean values of selected meteorological observations (source: German Weather Service DWD CDC [60]) during the measurement period (31 July to 3 October 2018), all nights ($n = 66$) and nights with calm and clear weather conditions ($n = 6$), T : air temperature.

	T (°C)	Precipitation (mm)	Cloud Cover (octas)	Sunshine (h)	Windspeed (m/s)
Measurement period	19.5	0.5	4.2	7.7	3.4
All nights	15.7	0.0	4.0	0.0	2.7
Nights with calm and clear weather conditions	18.1	0.0	1.0	0.0	2.7

Furthermore, Figure 3 displays the weather conditions during the measurement campaign, which can be described as hot and dry with long hours of sunshine (mean $T = 19.5$ °C). Seasonal changes are visible.

2.5. Data Processing

The following data processing was conducted for all nights, including the six nights with calm and clear weather conditions. We computed the arithmetic mean for RUR, URB and AGCs across the respective multiple stations. Then, mean T for each night (T_N) was calculated. Missing values occurred from 1 August to 8 August 2018 at station DAHF. Therefore, only values at station KANI were used to represent RUR in this period. In order to test for significant differences in T_N during all nights and the six selected nights, a Kruskal–Wallis Test [61] and a Dunn post-hoc test [62] were conducted for each AGC, Park1, Park2 and RUR. These non-parametric tests were used since the data are homoscedastic and not normally distributed for all stations during the nights with calm and clear weather conditions. Adjusted p-values were computed using the false discovery rate method according to Benjamini and Hochberg [63].

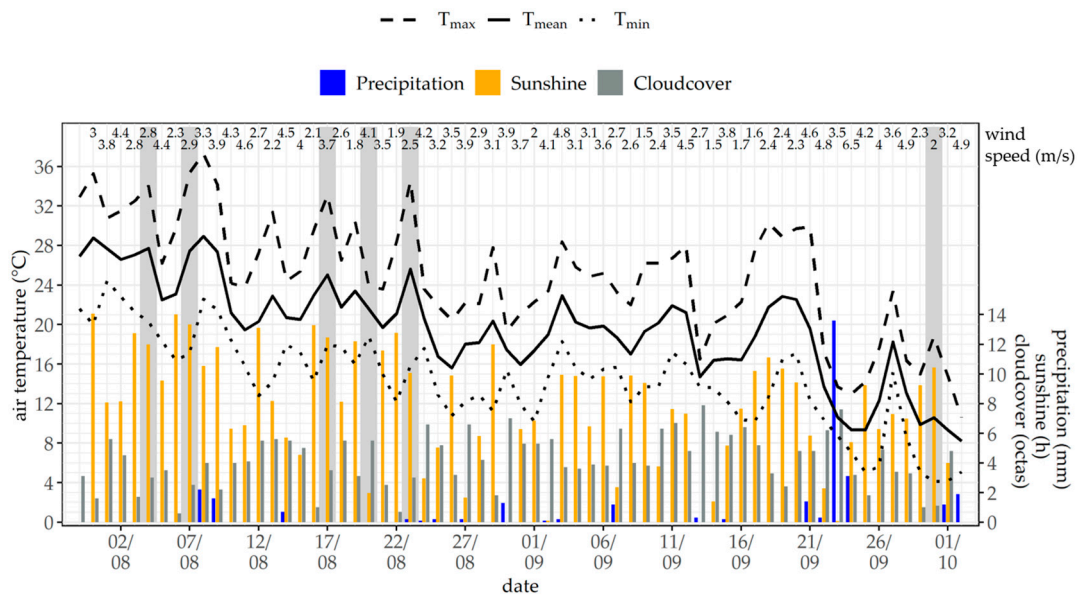


Figure 3. Weather conditions during the measurement campaign (daily values): minimum (T_{\min}), mean (T_{mean}) and maximum (T_{\max}) air temperature as lines on the left y -axis; cloud cover (mean), precipitation (sum), sunshine (sum) as bars on the right y -axis; wind speed (mean) as numbers (top). Selected nights with calm and clear weather conditions highlighted in gray, located at the day following the respective night (Source: German Weather Service DWD CDC [60]: Berlin–Tegel: cloud cover; Berlin–Tempelhof: all other variables).

Subsequently, the differences between URB and the other measurement stations (AGCs, both parks and RUR) were calculated. We applied the following Equation (1), where i represents all stations either each individual AGC, Park1, Park2 or RUR:

$$\Delta T_{N i} = T_{N i} - T_{N \text{ URB}} \quad (1)$$

Hereinafter, mean $\Delta T_{N i}$ are labeled as $\overline{\Delta T_{N i}}$. In order to address the second research question, multicollinearity between the calculated land surface characteristics (Table 1) was tested to identify the final selection of these characteristics. Accordingly, these five land surface characteristics were selected: shape complexity, size, FSI outside, distance to city center and sealing inside. Spearman’s rank-order correlation tests between $\overline{\Delta T_{N \text{ AGC}}}$ for each AGC and the aforementioned characteristics were carried out. This test is a nonparametric correlation test that uses the ranks of the data [64]. The correlation coefficient is hereinafter called r_s . The significance level for all statistical tests was set at $p \leq 0.05$.

3. Results

3.1. Nocturnal Air Temperature Differences

Concerning the first research question, Figure 4 shows $\Delta T_{N i}$ for each night, the average for nights with calm and clear weather conditions and all nights. $\Delta T_{N \text{ AGC}}$ of each individual AGC ($\Delta T_{N \text{ AGCi}}$) can be compared to $\Delta T_{N \text{ Park1}}$, $\Delta T_{N \text{ Park2}}$ and $\Delta T_{N \text{ RUR}}$. All $\Delta T_{N \text{ AGC}}$ and $\Delta T_{N \text{ RUR}}$ are statistically significant across all nights ($p \leq 0.05$), but not during nights with calm and clear weather conditions. On average, $\overline{\Delta T_{N \text{ AGC}}}$ amounts to -2.7 K during all nights and to -2.6 K during nights with calm and clear weather conditions. $\overline{\Delta T_{N \text{ AGCi}}}$ ranges from -3.7 K at AGC13 to -1.5 K at AGC2 during nights with calm and clear weather conditions and from -4.0 K at AGC11 to -1.6 K at AGC2 across all nights. During every single night $\Delta T_{N \text{ AGCi}}$ remained negative. In addition, two of the three AGCs with the shortest distances to the city center (AGC2 and AGC3) are also those with smallest $\Delta T_{N \text{ AGCi}}$ (-1.7 K to -1.5 K for calm and clear and all nights). Two AGCs with the largest distances to the city center

(AGC11 and AGC13) are those with largest $\overline{\Delta T_{N\ AGC_i}}$ (−3.6 K and −3.7 K for nights with calm and clear weather conditions; −4.0 K and −3.8 K for all nights). $\Delta T_{N\ AGC2}$, $\Delta T_{N\ AGC3}$, $\Delta T_{N\ AGC6}$ and $\Delta T_{N\ AGC8}$ have the smallest ranges, as they do not exceed 4.0 K during nights with calm and clear weather conditions. $\Delta T_{N\ AGC11}$ and $\Delta T_{N\ AGC13}$ show the widest range, exceeding 4.9 K.

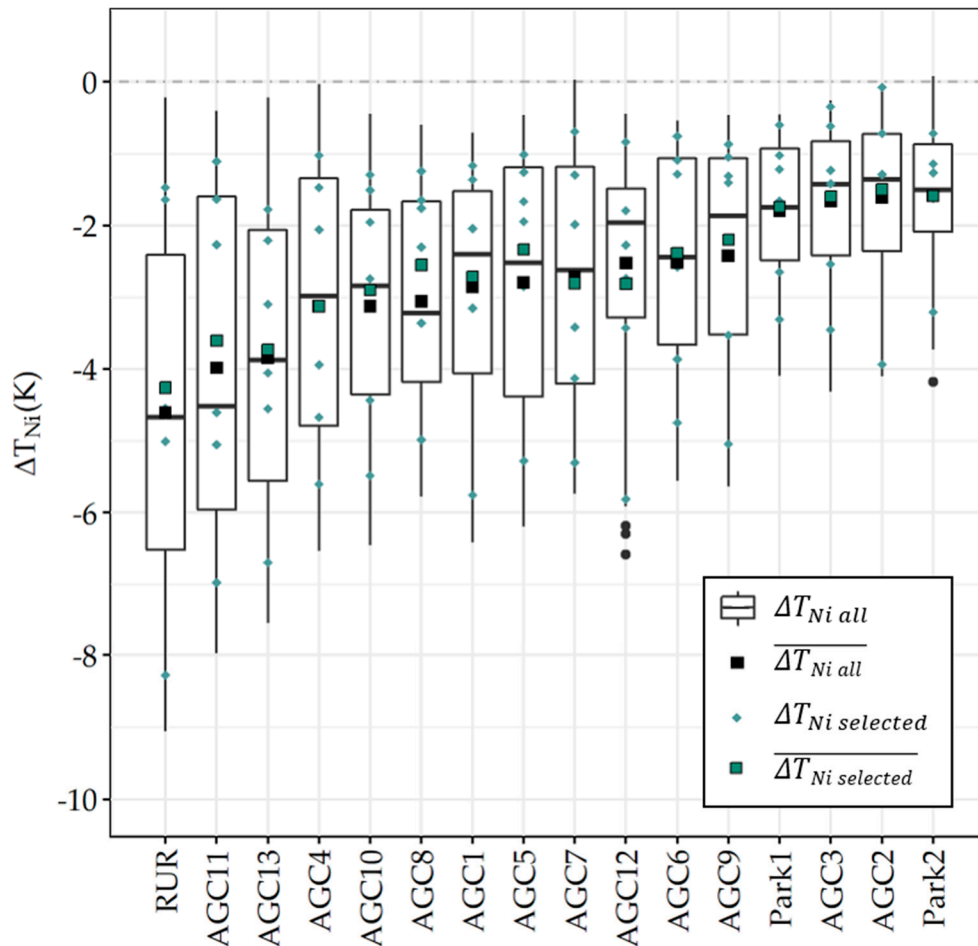


Figure 4. Mean air temperature differences to urban areas (URB) per night (ΔT_{N_i}) for all nights (boxplots, $n = 66$) and six nights with calm and clear weather conditions (blue diamonds) between URB and all allotment garden complexes (AGCs), rural areas (RUR) and both parks. Additionally, mean differences to URB (ΔT_{N_i}) during all nights are shown as black squares and as blue squares with a black outline for nights with calm and clear weather conditions. AGCs are sorted by $\Delta T_{N\ AGC}$ of all nights. Boxes range from 1st to 3rd quartile (inter quartile range–IQR), median is denoted as black line, whiskers range up to minimum/maximum value (maximum $1.5 \cdot IQR$), values below/above that range are denoted as black points.

For nights with calm and clear weather conditions $\overline{\Delta T_{N\ AGC_i}}$ is larger than $\overline{\Delta T_{N\ Park1}}$ and $\overline{\Delta T_{N\ Park2}}$, except $\overline{\Delta T_{N\ AGC2}}$ and $\overline{\Delta T_{N\ AGC3}}$. Across all nights all $\overline{\Delta T_{N\ AGC_i}}$ are larger $\overline{\Delta T_{N\ Park2}}$. The same applies to $\overline{\Delta T_{N\ AGC_i}}$ in comparison to $\overline{\Delta T_{N\ Park1}}$, except $\overline{\Delta T_{N\ AGC2}}$ and $\overline{\Delta T_{N\ AGC3}}$ (Figure 4). In contrast, none of the $\Delta T_{N\ AGC_i}$ were lower than $\Delta T_{N\ RUR}$ during nights with calm and clear weather conditions (−4.3 K) and during all nights (−4.6 K) (Figure 4).

The four nights with the largest ΔT_{N_i} , thus coldest compared to URB, occur at RUR (−8.2 K to −9.1 K on 31/07, 30/09, 12/09 and 06/08). $\Delta T_{N\ Park1}$ and $\Delta T_{N\ Park2}$ are similar to each other. Their ΔT_{N_i} differ 0.1 K, unaffected by the analyzed time frames.

T_N of URB during the whole measurement period was on average 17.4 °C across all nights. The nights with calm and clear weather conditions were slightly warmer with an average T_N of 19.7 °C.

3.2. Correlation between Land Surface Characteristics and Nocturnal Air Temperature Differences

Figures 5 and 6 depict the results of the correlation analyses. For nights with calm and clear weather conditions, the land surface characteristics FSI outside, size, distance to city center and shape complexity are all significantly ($p \leq 0.05$) correlated with $\overline{\Delta T_{N\ AGCi}}$. The correlation analysis for all nights produces insignificant correlations for all the characteristics, except for FSI outside (Figure 5b).

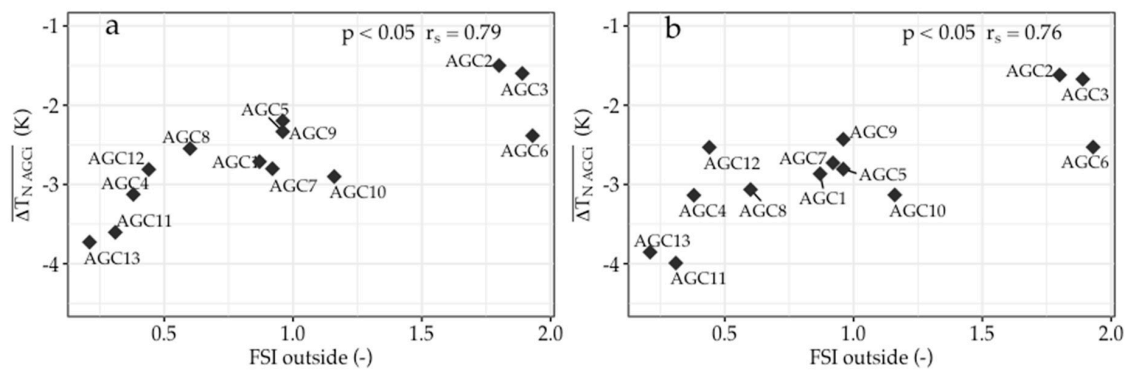


Figure 5. Correlations between $\overline{\Delta T_{N\ AGCi}}$ and the land surface characteristic ‘FSI outside’ for (a) nights with calm and clear weather conditions and (b) all nights of the measurement period. r_s : Spearman’s rank-order correlation coefficient; FSI outside: floor space index in a 500-m buffer around each allotment garden complex (AGC).

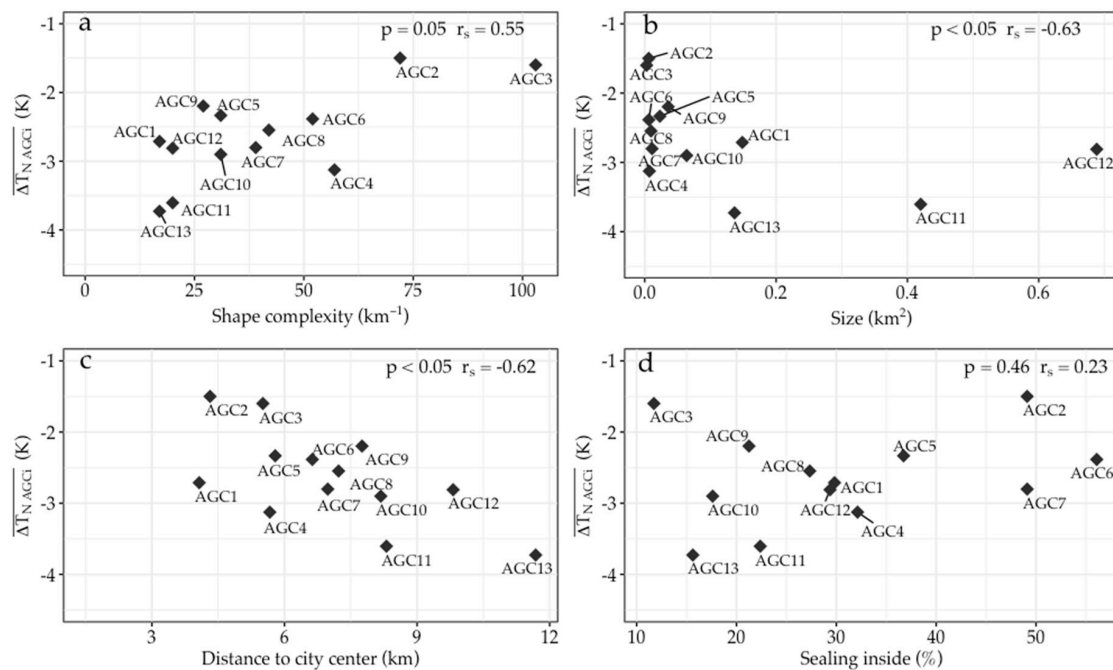


Figure 6. Correlations between $\overline{\Delta T_{N\ AGCi}}$ and land surface characteristics for nights with calm and clear weather conditions in Berlin: (a) shape complexity; (b) size; (c) distance to city center; (d) sealing inside. r_s : Spearman’s rank-order correlation coefficient; shape complexity: ratio between perimeter and size; sealing inside: degree of sealed land surfaces (including buildings) within each allotment garden complex (AGC).

FSI outside shows a significant ($p \leq 0.05$) positive correlation with $\overline{\Delta T_{N\ AGCi}}$ of $r_s = 0.79$ for nights with calm and clear weather conditions. The data for these nights suggests that a high FSI outside is accompanied by a small $\overline{\Delta T_{N\ AGCi}}$ (Figure 5a). The highest FSI outside occurs at AGC6 and AGC3 with 1.9, followed by AGC2 with 1.8, which are the AGCs with small $\overline{\Delta T_{N\ AGCi}}$. AGC2 and AGC3 are the

warmest AGCs of the sample group. AGC13 and AGC11, the AGCs with largest $\overline{\Delta T_{N\ AGC_i}}$, have the lowest FSI outside with 0.2 and 0.3, respectively. Taking all nights into account (Figure 5b), r_s between FSI outside and $\overline{\Delta T_{N\ AGC_i}}$ is lower than r_s for the nights with calm and clear weather conditions.

Shape complexity shows a significant positive correlation with $\overline{\Delta T_{N\ AGC_i}}$ of $r_s = 0.55$ for nights with calm and clear weather conditions. AGCs with a more complex shape, such as AGC2 and AGC3, show smaller $\overline{\Delta T_{N\ AGC_i}}$ (Figure 6a). The more complex the shape, the more space is adjacent to the surrounding built-up area. AGC1, AGC11, AGC12 and AGC13 represent the lowest complexity from $20\ \text{km}^{-1}$ to $17\ \text{km}^{-1}$, with AGC11 and AGC13 representing the coolest AGCs. The analysis of size of AGCs and $\overline{\Delta T_{N\ AGC_i}}$ results in a significant and strong negative correlation of $r_s = -0.63$ for nights with calm and clear weather conditions. Larger AGCs show lower T_N and so larger $\overline{\Delta T_{N\ AGC_i}}$. With 11 out of 13 sampled AGCs being smaller than $0.2\ \text{km}^2$, the land surface characteristic size displays a narrow range of values with the distribution being positively skewed (Figure 6b). Yet, this corresponds to the size distribution of all AGCs in Berlin (Appendix A).

The correlation between distance to the city center and $\overline{\Delta T_{N\ AGC_i}}$ also results in a significant and strong negative correlation ($r_s = -0.62$) for nights with calm and clear weather conditions. Figure 6c shows that the further the distance to the city center, the larger the $\overline{\Delta T_{N\ AGC_i}}$ and the cooler the AGCs.

There is no significant correlation found between sealing inside and $\overline{\Delta T_{N\ AGC_i}}$ (Figure 6d). Sealing inside also shows the smallest correlation coefficient of all the tested land surface characteristics ($r_s = 0.23$).

4. Discussion

4.1. Nocturnal Air Temperature Differences between AGCs and URB

Significant differences for all AGCs and RUR to URB across all nights confirm an intra-urban variability of $\overline{T_{N\ i}}$. These differences could be caused by the high heat storage capacity of the buildings and materials of the urban fabric, which absorb heat during daytime and release heat during night-time. Additionally, a relatively high SVF, as in AGCs and the low heat storage capacity of plants, lowers T_N [65,66]. Therefore, AGCs contribute to the variation of T_N in urban areas. This result is in line with previous studies about urban parks [32,56]. $\overline{\Delta T_{N\ AGC}}$ of $-2.7\ \text{K}$ can be compared to the PCI effect, which is rarely below $-3\ \text{K}$ and can vary, as a study of Spronken-Smith and Oke [14] shows. Correspondingly, AGCs can be understood as small cool spaces of local T_N minima inside the highly built-up city of Berlin.

PCI intensities increase in general from day to night [19]. In their review, Bowler et al. [16] showed that the average PCI is about $0.2\ \text{K}$ higher at night than during daytime. Similarly, Fenner et al. [56] demonstrated that differences during the day- and night-time at Park1 compared to one of the rural sites (DAHF) are more pronounced during summer time than in winter time. An analogous effect could be expected for AGCs. Further investigations with data for longer time periods in several seasons, as well as during day and night are needed to confirm this hypothesis.

Another subject of research is the cooling ability of AGCs for their immediate surroundings, similar to investigations of the PCI effect and its range of influence [11,25,59,67]. Schlegelmilch [43] was able to demonstrate a cooling effect of AGC10 on its surroundings. However, the measurement setup of the current study does not allow a general statement about the cooling effect on the surroundings of AGCs. Therefore, future studies could perform detailed measurements in the surrounding areas of each AGC or use high-resolution numerical simulations with meso-scale models [68] or large-eddy simulations [69,70].

Even though the differences in $\overline{T_N}$ for individual AGCs were not found to be statistically significant from URB during nights with calm and clear weather conditions, urban areas in Berlin are warmer than the sampled AGCs. Other studies about urban green infrastructure found that calm and dry weather enhances local effects and night-time UHI [14,25]. However, a large range in ΔT_N was found for the

selected six nights. Even under these relatively similar conditions, cooling processes still produce a high ΔT_N variability.

The rain event in the measurement period of this study led to some of the smallest $\Delta T_{N\ AGCi}$. After the rain event, it is possible that all areas were able to provide evaporative cooling during the day, affecting their T_N in a way similar to frequently irrigated AGCs.

To date, climatic studies concerning irrigation in AGCs and urban parks are few in number. Egerer et al. [27] found that irrigation was not a sufficient factor to predict T of AGs in their study. Non-representative interviews with the tenants of AGC plots in our study show that the amount and regularity of irrigation differs highly. It was not possible to quantify the amount of irrigation for each AGC during the measurement period. It would have required a representative and systematic survey of each tenant's irrigation habits or measuring the amount of water used for irrigation. This was beyond the scope of this study. However, acquisition of information about irrigation could be accomplished by future studies involving citizen science. Such efforts should be accompanied by measurements of, e.g., atmospheric humidity or latent heat fluxes to provide more insights into effects of evapotranspirative cooling within AGCs.

4.2. Nocturnal Air Temperature Differences between AGCs, Urban Parks and RUR

During the day, tall and densely planted trees are known as the main driver of vegetative cooling through shading and evapotranspiration [16,71]. However, at night trees store heat under their canopies and thus prevent exchange with cooler air masses [16]. Since there are few or no tall trees in the AGCs in Berlin, due to legal restrictions [41], $\overline{\Delta T_{N\ AGCi}}$ of at least 11 out of the 13 sampled AGCs is larger (during both calm and clear and all nights) than $\overline{\Delta T_{N\ Park1}}$. Park1 has a low SVF, due to dense and tall trees. Fenner et al. [56] showed similar outcomes for T_N of Park1 compared to the rural station DAHF.

The former airport Park2, has only a few large trees and is dominated by grassland and old runways with a high SVF. Its vegetative structure resembles more the structure of AGCs than the one of Park1. Open park structures as in Park2 lead to a low heat storage capacity and should therefore result in high nocturnal cooling [2]. Quanz et al. [59] also show that Park2 has a cooling effect on its surroundings. It is therefore remarkable that almost all sampled AGCs, even very small ones such as AGC4 and AGC8, show larger $\overline{\Delta T_{N\ i}}$ than Park2 (Figure 4). Park 2 is more than three times larger than the largest AGC (AGC12, cf. Appendix B). Reasons for $\overline{\Delta T_{N\ i}}$ differences between Park2 and AGCs may lie in the varying degrees of maintenance, e.g., Park2 is rarely irrigated, whereas AGCs are frequently and intensively irrigated. This favors evapotranspirative cooling during the day, similar to urban gardens, as shown by Egerer et al. [27]. Increased evapotranspiration through irrigation around sunset can result in a higher cooling potential at night [19]. Moreover, Park2 is characterized by large asphalt areas and has a high FSI outside (see Appendix B), which could be one reason why $\overline{\Delta T_{N\ Park2}}$ is smaller than $\overline{\Delta T_{N\ AGC}}$ [71,72]. Additionally, the position of its measurement station near the south edge of the park (around 200 m to its border) could enhance the effect of built-up surroundings on T_{Ni} .

Furthermore, the large-scale UHI is more pronounced at both selected parks (mean of 3.0 K) due to their central location in Berlin (mean distance to city center 3.9 km, see Figure 2), than the one of the AGCs (mean of 1.8 K). AGCs are located on average 7.1 km away from the city center. Thus, in the hot and dry summer of 2018, higher T_N occurred in both parks compared to the AGCs. Different percentages and varieties of vegetation cover, as well as the imperviousness and the intensity of irrigation may have all contributed to varied T_N . This is confirmed by Edmondson et al. [36], Schwarz et al. [73] and Egerer et al. [27] for urban parks and urban gardens, respectively.

It is noteworthy that both parks differ only slightly in their $\overline{\Delta T_{N\ i}}$, despite having different characteristics (dense trees vs. grassland; Appendix B). It seems that other factors overshadow the influence of the parks' characteristics.

The nocturnal UHI effect for the city of Berlin can clearly be observed in $\overline{\Delta T_N}$ of RUR (4.6 K across all nights). This is in line with previous studies for Berlin [4,56,59]. Due to the location and structure of the AGCs (e.g., higher FSI outside than rural areas), they are more influenced by the urban

environment than RUR. This is demonstrated by the larger $\overline{\Delta T_{N\text{RUR}}}$ compared to the $\overline{\Delta T_{N\text{AGC}}}$. Thus, we can conclude that T_N of AGCs are influenced by their surrounding built-up areas (Figure 5) and the large-scale nocturnal UHI of Berlin [4,56].

4.3. Land Surface Characteristics

The correlation analysis shows that all investigated land surface characteristics except sealing inside correlated significantly with $\overline{\Delta T_{N\text{AGCi}}}$ for nights with calm and clear weather conditions. While across all nights, only FSI outside resulted in a significant correlation with $\overline{\Delta T_{N\text{AGCi}}}$.

FSI outside demonstrated the strongest correlation with $\overline{\Delta T_{N\text{AGCi}}}$. As FSI outside decreases, $\overline{\Delta T_{N\text{AGCi}}}$ increases. Stored heat is emitted from sealed surfaces and built-up areas, impacting their surroundings, especially at night [74]. The influence of the surroundings on urban gardens was studied by Egerer et al. [27] and by Lin et al. [26]. They concluded that the surrounding environment had an influence on the gardens, i.e., UHI effects were more visible in gardens with densely built-up surroundings than in gardens with less built-up surroundings. The same effect of the surroundings on AGCs was found in the present study. Future studies could survey specific characteristics of the surroundings of AGCs more in detail, e.g., the height distribution, colors and materials of buildings.

Beside the built-up structure of the surroundings of AGCs, shape complexity correlated significantly with $\overline{\Delta T_{N\text{AGCi}}}$ for nights with calm and clear weather conditions. A more complex shape may lead to greater influence from the surrounding area, resulting in an increased T_N . This is also stated by Lin et al. [26]. For urban parks in Berlin, Dugord et al. [9] found a similar result, using land surface temperatures. They state that large and complex-shaped forested spaces, as well as interconnected and spatially aggregated urban green spaces, greatly reduce night-time land surface temperatures. However, the comparison of land surface temperature with T is not trivial.

The land surface characteristic size showed a significant strong negative correlation with $\overline{\Delta T_{N\text{AGCi}}}$ during nights with calm and clear weather conditions. Several studies on urban parks found similar results [14,16,25]. However, other studies did not find a relationship between size and T_N for urban parks [16]. Our analysis also shows that the largest investigated AGC (AGC12) is not the coolest AGC. This could be explained by its FSI outside, shape complexity, sealing inside or further characteristics which have not been examined yet.

The correlation between $\overline{\Delta T_{N\text{AGCi}}}$ and the distance to the city center was strong and negative. Therefore, the influence of the large-scale nocturnal UHI effect becomes visible. Dugord et al. [9] also found a negative correlation between the land surface temperature of urban areas and the distance to city center in Berlin (the same center as chosen for this study).

Sealing inside showed no significant correlation with $\overline{\Delta T_{N\text{AGCi}}}$, suggesting that the degree of sealing within the AGCs does not have an influence on their T_N . On a larger scale, it has been confirmed by many studies [42,75–77] that the higher the proportion of sealing and the lower the proportion of vegetation in a city, the more pronounced the UHI effect. However, in this study, the characteristic sealing inside may be overshadowed by previously discussed characteristics of AGCs. Additionally, not investigated characteristics, such as plant choices and types of vegetation management (e.g., degree of fertilizing or pruning) could be influential. Vieira et al. [71] also found that the type of management, plant choices and the structure of the vegetation have an influence on urban gardens' T . These possibly influential land surface characteristics were beyond the scope of this study and could be investigated in future studies.

5. Conclusions

The present study was carried out during two months of the summer of 2018 and analyzed 13 of 555 AGCs in Berlin. The study delivers findings on the effect of AGCs on the microclimate of Berlin. All AGCs analyzed were shown to be cooler than URB during calm, dry and cloudless nights, as well as across all nights, during the measurement period from July to October 2018. Furthermore, AGCs provide a climate regulating ES of night-time T reduction. The extent of this reduction is higher or

at least the same as provided by large urban parks in Berlin. The cooling effect of AGCs may be comparable to the PCI effect.

This study shows that AGs, as a part of the urban green infrastructure of Berlin, not only serve as biodiversity hotspots [40] or places of social interaction [35], but also support the climatic regulation of the city. This should be considered by policy makers and urban planners, especially considering the declining number of AGs in Berlin. AGs could contribute to achieving the EU 2020 objective of reversing the loss of ESs [78].

The sampled AGCs show smaller $\overline{\Delta T_{N\ AGCi}}$ than the overall night-time UHI intensity of Berlin, i.e., $\Delta T_{N\ RUR}$. Hence, it can be assumed that they are influenced by the large-scale UHI of Berlin due to their location within built-up urban areas.

Moreover, AGCs are influenced by their micro-scale land surface characteristics. Given the significant correlation between $\overline{\Delta T_{N\ AGCi}}$ and FSI outside, it can be concluded that a high level of built-up density in the surroundings of an AGC is associated with a small $\overline{\Delta T_{N\ AGCi}}$. This means that those AGCs show higher T_{Ni} . Heat absorbed during the day by the built-up area is released during the night and influences AGCs in the immediate vicinity. Furthermore, the results of the correlation analysis show that $\overline{\Delta T_{N\ AGCi}}$ is positively influenced by the size and distance to the city center. This confirms results of previous studies about urban parks and urban gardens. The shape complexity of AGCs also correlates significantly with $\overline{\Delta T_{N\ AGCi}}$, though this correlation is less strong. To summarize, the investigated AGCs are mainly influenced by the surrounding land surface characteristics. Characteristics of or within AGCs are still important but seem to have a minor impact on $\overline{\Delta T_{N\ AGCi}}$.

In order to strengthen these initial findings about the influence of the examined land surface characteristics and about the general microclimatic behavior of AGCs, further investigations would be highly valuable. These investigations should include, e.g., a higher number of AGCs, other cities, measurements during daytime and different seasons, as well as an analysis of potential irrigation effects on evapotranspirative cooling.

Author Contributions: A.T.R., V.L., C.S. and L.M. conceived, designed and performed the measurement campaign; A.T.R., V.L. and C.S. analyzed the data; A.T.R., V.L., C.S. and L.M. wrote the manuscript; D.F., F.M. and M.O. contributed to the development of the study design, prepared existing measurement data from Technische Universität Berlin and contributed to reviewing and writing of the manuscript. All authors interpreted and discussed the results. All authors have read and agreed to the published version of the manuscript.

Funding: D.F. received financial support from the Deutsche Forschungsgemeinschaft (DFG) as part of the research project ‘Heat waves in Berlin, Germany—urban climate modifications’ (Grant No. SCHE 750/15-1). The study contributes to the research program ‘Urban Climate Under Change ([UC]²)’, and to ‘Research for Sustainable Development’ (FONA), within the research project ‘Three-dimensional observation of atmospheric processes in cities (3DO)’, funded by the German Federal Ministry of Research and Education (Grant No. FKZ 01LP1602).

Acknowledgments: This research resulted from a master’s project named “From Surface to Space” and we are grateful to all participants for supporting the measurement campaign, especially Anahita Bidjanbeg. Thanks to the department of plant ecology, especially Andreas Lemke, who provided us with the necessary measuring equipment. We also thank Moritz Münch, Katja Kowalski, Freya Watkins and Frances Foley for their helpful advice. We further thank Hartmut Küster and Ingo Suchland for maintaining the weather stations of the Technische Universität Berlin. Finally, we would especially like to thank all allotment gardeners who allowed us to perform the measurements in their private garden plots. We acknowledge support by the German Research Foundation and the Open Access Publication Fund of TU Berlin.

Conflicts of Interest: The authors declare no conflict of interest.

Appendix A

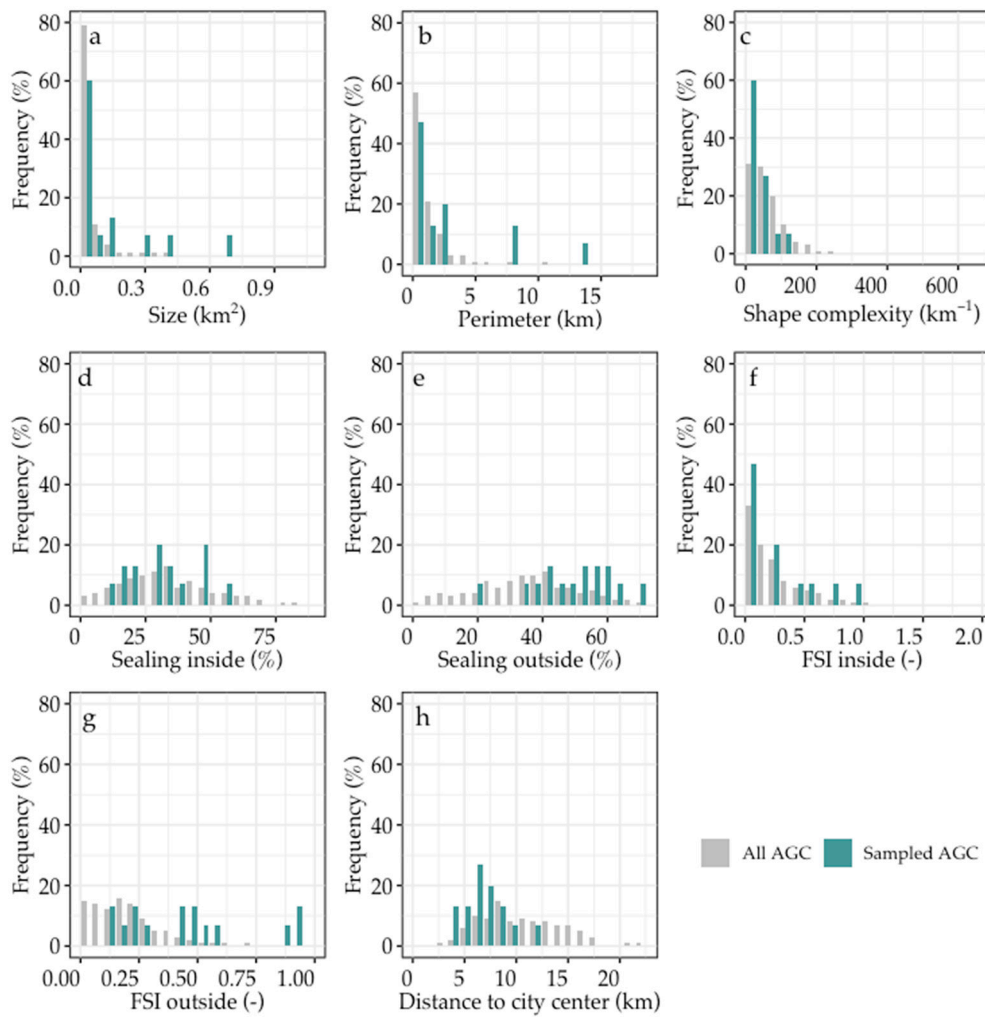


Figure A1. Distributions of the selected land surface characteristics of all allotment garden complexes (AGCs) in Berlin and sampled AGCs ($n = 13$): (a) size; (b) perimeter; (c) shape complexity; (d) sealing inside; (e) sealing outside; (f) FSI inside; (g) FSI outside; (h) distance to the city center. Shape complexity: ratio between perimeter and size, FSI: floor space index, inside and outside: land surface characteristic of the AGCs themselves and in a 500-m buffer around each AGC, respectively.

Appendix B

Table A1. Location and description of all measurement stations, mean night-time air temperature (T_N) and mean difference in night-time air temperature to URB ($\overline{\Delta T_N}$) for all nights and nights of calm and clear weather conditions (selected). Sky view factor (SVF) values are spatial means for a 250 m radius from Fenner et al. [4]. Shape complexity: ratio between perimeter and size, FSI: floor space index, inside and outside: land surface characteristic of the AGCs themselves and in a 500-m buffer around each AGC, respectively, LCZ: local Climate Zone

ID	RUR		Park1	Park2	URB		
Station	Kaniswall, KANI	Dahlemer Feld, DAHF	Tiergarten	Tempelhofer Feld	Alexanderplatz, ALEX	Bamberger Straße, BAMB	Dessauer Straße, DESS
Operator	DWD	TUB	TUB	DWD	DWD	TUB	TUB
Latitude/Longitude	52.4040 N/13.7309 E	52.4777 N/13.2252 E	52.5145 N/13.3636 E	52.4675 N/13.4021 E	52.5198 N/13.4054 E	52.4964 N/13.3375 E	52.5045 N/13.3783 E
Site elevation (m)	33.0	51.0	34.0	48.0	36.0	36.0	33.5
Size (km ²)	–	–	2.1	3.0	–	–	–
Perimeter (km)	–	–	22.63	7.34	–	–	–
Shape complexity (km ⁻¹)	–	–	0.09	0.41	–	–	–
Distance to city center (km)	25.0	13.1	3.0	4.9	0.0	5.5	2.6
FSI inside/outside (-)	-/0.00	-/0.74	0.06/0.36	0.12/0.36	-/0.74	-/2.37	-/1.69
Sealing in-/outside (%)	-/1.50	-/0.0	6.18/42.46	24.66/35.33	-/73.43	-/70.07	-/61.48
LCZ		B	A	D		2	
SVF (-)	0.9	0.46	0.16	0.96	0.54	0.24	0.42
T_N (selected) (°C)		15.5	18.0	18.1		19.7	
T_N (all) (°C)		12.8	15.9	15.7		17.4	
$\overline{\Delta T_N}$ (selected) (K)		-4.3	-1.7	-1.6		–	
$\overline{\Delta T_N}$ (all) (K)		-4.6	-1.8	-1.6		–	
max/min ΔT_N (selected) (K)		-1.5/-8.3	-0.6/-3.3	-0.7/-3.2		–	
max/min ΔT_N (all) (K)		-0.2/-9.1	-0.5/-4.1	0.1/-4.2		–	

Table A2. Location and description of all allotment garden complexes (AGCs), mean night-time air temperature (T_N) and mean difference in night-time air temperature to URB ($\overline{\Delta T_N}$) for all nights and nights of calm and clear weather conditions (selected). Sky view factor (SVF) values for AGCs derived from fish-eye photos. Shape complexity: ratio between perimeter and size, FSI: floor space index, inside and outside: land surface characteristic of the AGCs themselves and in a 500-m buffer around each AGC, respectively.


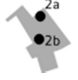
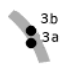
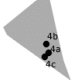
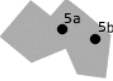
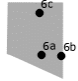

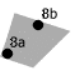
ID	AGC1			AGC2		AGC3		AGC4		
Logger ID	1a	1b	1c	2a	2b	3a	3b	4a	4b	4c
Latitude/Longitude	52.56519 N/13.404214 E	52.557609 N/13.404278 E	52.556801 N/13.404211 E	52.544499 N/13.357116 E	52.544136 N/13.357093 E	52.526632 N/13.260129 E	52.523865 N/13.325949 E	52.499702 N/13.483952 E	52.499840 N/13.483896 E	52.499641 N/13.483865 E
Shape										
Scale	1:35,000			1:8500		1:10,000		1:8500		
Site elevation (m)	46.5			36.5		33.5		34.5		
Size (km ²)	0.15			0.006		0.003		0.007		
Perimeter (km)	2.55			0.44		0.3		0.4		
Shape complexity (km ⁻¹)	17.1			71.8		103.2		56.7		
Distance to city center (km)	4.1			4.3		5.5		5.7		
FSI in-/outside (-)	0.01/0.87			0.78/1.80		0.00/1.89		0.00/0.38		
Sealing in-/outside (%)	29.82/49.61			49.11/61.84		11.73/71.13		32.12/46.88		
SVF (-)	0.93	0.8	0.71	0.91	0.77	0.79	0.74	0.93	0.92	0.86
T_N (selected) (°C)	17.0			18.2		18.1		16.6		
T_N (all) (°C)	14.5			15.8		15.7		14.3		
$\overline{\Delta T_N}$ (selected) (K)	-1.7			-1.5		-1.6		-3.1		
$\overline{\Delta T_N}$ (all) (K)	-2.9			-1.6		-1.7		-3.1		
max/min ΔT_N (selected) (K)	-1.2/-5.8			-0.1/-3.9		-0.3/-3.5		-1.0/-5.6		
max/min ΔT_N (all) (K)	-0.7/-6.4			-0.1/-4.1		-0.3/-4.3		0.0/-6.5		
ID	AGC5		AGC6			AGC7		AGC8		
Logger ID	5a	5b	6a	6b	6c	7a	7b	8a	8b	
Latitude/Longitude	52.476465 N/13.453303 E	52.476300 N/13.454340 E	52.522476 N/13.272697 E	52.483948 N/13.329340 E	52.484454 N/13.328883 E	52.506701 N/13.506705 E	52.506472 N/13.507516 E	52.565796 N/13.331121 E	52.566356 N/13.332066 E	
Shape										
Scale	1:10,000		1:10,000			1:10,000		1:10,000		
Site elevation (m)	33.5		36.5			38		57.75		
Size (km ²)	0.02		0.006			0.011		0.01		
Perimeter (km)	0.71		0.33			0.44		0.4		

Table A2. Cont.









ID	AGC5		AGC6		AGC7		AGC8		
Shape complexity (km ⁻¹)	30.8		51.5		39.4		42.3		
Distance to city center (km)	5.8		6.6		7.0		7.2		
FSI in-/outside (-)	0.46/0.96		2.00/1.93		0.56/0.92		0.27/0.60		
Sealing in-/outside (%)	36.73/57.56		56.08/60.55		49.12/50.8		27.34/42.23		
SVF (-)	0.76	0.9	0.51	0.81	0.8	0.85	0.59	0.82	0.89
T _N (selected) (°C)	17.4		17.4		16.9		16.2		
T _N (all) (°C)	14.6		14.9		14.7		14.4		
$\overline{\Delta T_N}$ (selected) (K)	-2.3		-2.4		-2.8		-2.5		
$\overline{\Delta T_N}$ (all) (K)	-2.8		-2.5		-2.7		-3.1		
max/min ΔT_N (selected) (K)	-1.0/-5.3		-0.8/-4.7		-0.7/-5.3		-1.2/-5.0		
max/min ΔT_N (all) (K)	-0.5/-6.2		-0.5/-5.6		0.0/-5.7		-0.6/-5.8		
ID	AGC9			AGC10			AGC11		
Logger ID	9a	9b	9c	10a	10b	10c	11a	11b	11c
Latitude/Longitude	52.487628 N/13.307651 E	52.487071 N/13.306620 E	52.486057 N/13.305941 E	52.474764 N/13.311752 E	52.473863 N/13.312507 E	52.474095 N/13.313315 E	52.456609 N/13.474660 E	52.456151 N/13.474205 E	52.456078 N/13.464090 E
Shape									
Scale	1:20,000			1:20,000			1:40,000		
Site elevation (m)	44.5			41.2			33.83		
Size (km ²)	0.04			0.06			0.42		
Perimeter (km)	0.96			1.98			8.33		
Shape complexity (km ⁻¹)	26.9			31.0			19.8		
Distance to city center (km)	7.8			8.2			8.3		
FSI in-/outside (-)	0.00/0.96			0.26/1.16			0.02/0.31		
Sealing in-/outside (%)	21.25/56.76			17.61/50.67			22.38/32.73		
SVF (-)	0.86	0.75	0.94	0.92	0.92	0.72	0.92	0.96	0.82
T _N (selected) (°C)	17.5			16.8			16.1		
T _N (all) (°C)	15.0			14.3			13.4		
$\overline{\Delta T_N}$ (selected) (K)	-2.2			-2.9			-3.6		
$\overline{\Delta T_N}$ (all) (K)	-2.4			-3.1			-4.0		
max/min ΔT_N (selected) (K)	-0.9/-5.0			-1.3/- 5.5			-1.1/-7.0		
max/min ΔT_N (all) (K)	-0.5/-5.6			-0.4/-6.5			-0.4/-8.0		

Table A2. Cont.

ID	AGC12				AGC13			
Logger ID	12a	12b	12c	12d	12e	13a	13b	
Latitude/Longitude	52.523609 N/13.325962 E	52.526377 N/13.267863 E	52.522101 N/13.271471 E	52.483956 N/13.328949 E	52.522335 N/13.269297 E	52.529149 N/13.578040 E	52.530704 N/13.580143 E	
Shape								
Scale	1:40,000				1:40,000			
Site elevation (m)	52.2				50			
Size (km ²)	0.69				0.14			
Perimeter (km)	13.91				2.27			
Shape complexity (km ⁻¹)	20.2				16.6			
Distance to city center (km)	9.8				11.7			
FSI in-/outside (-)	0.03/0.44				0.00/0.21			
Sealing in-/outside (%)	29.37/37.19				15.63/19.45			
SVF (-)	0.93	0.91	0.9	0.79	0.85	0.95	0.72	
T _N (selected) (°C)	16.9				16.0			
T _N (all) (°C)	14.9				13.6			
$\overline{\Delta T_N}$ (selected) (K)	-2.8				-3.7			
$\overline{\Delta T_N}$ (all) (K)	-2.5				-3.8			
max/min ΔT_N (selected) (K)	-0.8/-5.8				-1.8/-6.7			
max/min ΔT_N (all) (K)	-0.4/-6.6				-0.2/-7.5			

Appendix C

Table A3. Excluded measurement sites in allotment garden complexes (AGCs) with the description of the location and the reason for the exclusion.

ID	AGCx		AGCy	AGC12
Logger ID	Xa	Xb	Ya	12f
Shape				
Scale	1:400,000		1:100,000	1:40,000
Latitude/Longitude	52.478976 N/13.467163 E	52.479141 N/13.466929 E	52.522476 N/13.272697 E	52.523577 N/13.269642 E
Reason for the exclusion of the data	Missing data: 81%		Missing data: 49%	Missing data: 21%
	Exclusion of Xa led to exclusion of AGCx, because the minimum number of two measurement stations per AGC was not provided.			

Data about air temperature of all sampled AGCs and the measurement stations DAHF, DESS, BAMB and TIER is freely available online under: <http://dx.doi.org/10.14279/depositonce-9881.2>. Data about the measurement stations TEMP and KANI is freely available under https://opendata.dwd.de/climate_environment/CDC/observations_germany/climate/hourly/air_temperature/recent/. Data about the measurement station ALEX is freely available under: https://opendata.dwd.de/climate_environment/CDC/observations_germany/climate_urban/hourly/air_temperature/recent/. Data about the land surface characteristics are freely available from the environmental atlas of the Senate Department for Urban Development and Housing, Berlin; FSI: Geoportal Berlin/Städtebauliche Dichte - Geschossflächenzahl (GFZ) 2019: https://fbinter.stadt-berlin.de/fb/index.jsp?loginkey=showMap&mapId=wmsk01_02versieg2016@senstadt; Size, Perimeter, Distance to the measurement station ALEX: Geoportal Berlin/Kleingartenbestand Berlin: https://fbinter.stadt-berlin.de/fb/index.jsp?loginkey=showMap&mapId=wmsk01_02versieg2016@senstadt; Sealing: Geoportal Berlin/Versiegelung 2016: https://fbinter.stadt-berlin.de/fb/index.jsp?loginkey=showMap&mapId=wmsk01_02versieg2016@senstadt.

References

- Gill, S.E.; Handley, J.F.; Ennos, A.R.; Pauleit, S. Adapting Cities for Climate Change: The Role of the Green Infrastructure. *Built Environ.* **2007**, *33*, 115–133. [[CrossRef](#)]
- Oke, T.R. The energetic basis of the urban heat island. *Q. J. R. Meteorol. Soc.* **1982**, *108*, 1–24. [[CrossRef](#)]
- Arnfield, A.J. Two decades of urban climate research: A review of turbulence, exchanges of energy and water, and the urban heat island. *Int. J. Clim.* **2003**, *23*, 1–26. [[CrossRef](#)]
- Fenner, D.; Meier, F.; Bechtel, B.; Otto, M.; Scherer, D. Intra and inter ‘local climate zone’ variability of air temperature as observed by crowdsourced citizen weather stations in Berlin, Germany. *Meteorol. Z.* **2017**, *26*, 525–547. [[CrossRef](#)]
- Oke, T.R. Street design and urban canopy layer climate. *Energy Build.* **1988**, *11*, 103–113. [[CrossRef](#)]
- Stewart, I.D.; Oke, T.R. Local Climate Zones for Urban Temperature Studies. *Bull. Am. Meteorol. Soc.* **2012**, *93*, 1879–1900. [[CrossRef](#)]
- Alexander, P.; Mills, G. Local Climate Classification and Dublin’s Urban Heat Island. *Atmosphere* **2014**, *5*, 755–774. [[CrossRef](#)]
- Mills, G. Luke Howard and The Climate of London. *Weather* **2008**, *63*, 153–157. [[CrossRef](#)]
- Dugord, P.-A.; Lauf, S.; Schuster, C.; Kleinschmit, B. Land use patterns, temperature distribution, and potential heat stress risk—The case study Berlin, Germany. *Comput. Environ. Urban* **2014**, *48*, 86–98. [[CrossRef](#)]

10. Lauf, S.; Haase, D.; Kleinschmit, B. Linkages between ecosystem services provisioning, urban growth and shrinkage—A modeling approach assessing ecosystem service trade-offs. *Ecol. Indic.* **2014**, *42*, 73–94. [[CrossRef](#)]
11. Doick, K.J.; Peace, A.; Hutchings, T.R. The role of one large greenspace in mitigating London’s nocturnal urban heat island. *Sci. Total Environ.* **2014**, *493*, 662–671. [[CrossRef](#)] [[PubMed](#)]
12. Emmanuel, R.; Loconsole, A. Green infrastructure as an adaptation approach to tackling urban overheating in the Glasgow Clyde Valley Region, UK. *Landsc. Urban Plan.* **2015**, *138*, 71–86. [[CrossRef](#)]
13. Chang, C.-R.; Li, M.-H.; Chang, S.-D. A preliminary study on the local cool-island intensity of Taipei city parks. *Landsc. Urban Plan.* **2007**, *80*, 386–395. [[CrossRef](#)]
14. Spronken-Smith, R.A.; Oke, T.R. The thermal regime of urban parks in two cities with different summer climates. *Int. J. Remote Sens.* **1998**, *19*, 2085–2104. [[CrossRef](#)]
15. Zardo, L.; Geneletti, D.; Pérez-Soba, M.; van Eupen, M. Estimating the cooling capacity of green infrastructures to support urban planning. *Ecosyst. Serv.* **2017**, *26*, 225–235. [[CrossRef](#)]
16. Bowler, D.E.; Buyung-Ali, L.; Knight, T.M.; Pullin, A.S. Urban greening to cool towns and cities: A systematic review of the empirical evidence. *Landsc. Urban Plan.* **2010**, *97*, 147–155. [[CrossRef](#)]
17. Larondelle, N.; Haase, D. Urban ecosystem services assessment along a rural–urban gradient: A cross-analysis of European cities. *Ecol. Indic.* **2013**, *29*, 179–190. [[CrossRef](#)]
18. Höpfe, P. Improving indoor thermal comfort by changing outdoor conditions. *Energy Build.* **1991**, *16*, 743–747. [[CrossRef](#)]
19. Spronken-Smith, R.A.; Oke, T.R. Scale Modelling of Nocturnal Cooling in Urban Parks. *Bound. Layer Meteorol.* **1999**, *93*, 287–312. [[CrossRef](#)]
20. Ren, Z.; He, X.; Zheng, H.; Zhang, D.; Yu, X.; Shen, G.; Guo, R. Estimation of the Relationship between Urban Park Characteristics and Park Cool Island Intensity by Remote Sensing Data and Field Measurement. *Forests* **2013**, *4*, 868–886. [[CrossRef](#)]
21. Cao, X.; Onishi, A.; Chen, J.; Imura, H. Quantifying the cool island intensity of urban parks using ASTER and IKONOS data. *Landsc. Urban Plan.* **2010**, *96*, 224–231. [[CrossRef](#)]
22. Feyisa, G.L.; Dons, K.; Meilby, H. Efficiency of parks in mitigating urban heat island effect: An example from Addis Ababa. *Landsc. Urban Plan.* **2014**, *123*, 87–95. [[CrossRef](#)]
23. Hagishima, A.; Narita, K.-I.; Tanimoto, J. Field experiment on transpiration from isolated urban plants. *Hydrol. Process.* **2007**, *21*, 1217–1222. [[CrossRef](#)]
24. Meier, F.; Scherer, D. Spatial and temporal variability of urban tree canopy temperature during summer 2010 in Berlin, Germany. *Theor. Appl. Clim.* **2012**, *110*, 373–384. [[CrossRef](#)]
25. Upmanis, H.; Eliasson, I.; Lindqvist, S. The influence of green areas on nocturnal temperatures in a high latitude city (Göteborg, Sweden). *Int. J. Clim.* **1998**, *18*, 681–700. [[CrossRef](#)]
26. Lin, B.B.; Egerer, M.H.; Liere, H.; Jha, S.; Bichier, P.; Philpott, S.M. Local- and landscape-scale land cover affects microclimate and water use in urban gardens. *Sci. Total Environ.* **2018**, *610–611*, 570–575. [[CrossRef](#)]
27. Egerer, M.H.; Lin, B.B.; Threlfall, C.G.; Kendal, D. Temperature variability influences urban garden plant richness and gardener water use behavior, but not planting decisions. *Sci. Total Environ.* **2019**, *646*, 111–120. [[CrossRef](#)]
28. Zölch, T.; Maderspacher, J.; Wamsler, C.; Pauleit, S. Using green infrastructure for urban climate-proofing: An evaluation of heat mitigation measures at the micro-scale. *Urban For. Urban Green.* **2016**, *20*, 305–316. [[CrossRef](#)]
29. Koc, C.B.; Osmond, P.; Peters, A. Towards a comprehensive green infrastructure typology: A systematic review of approaches, methods and typologies. *Urban Ecosyst.* **2017**, *20*, 15–35. [[CrossRef](#)]
30. Bell, S.; Fox-Kämper, R.; Keshavarz, N.; Benson, M.; Caputo, S.; Noori, S.; Voigt, A. (Eds.) *Urban Allotment Gardens in Europe*; Routledge: London, UK; New York, NY, USA, 2018; ISBN 978-1-138-92109-2.
31. Cabral, I.; Keim, J.; Engelmann, R.; Kraemer, R.; Siebert, J.; Bonn, A. Ecosystem services of allotment and community gardens: A Leipzig, Germany case study. *Urban For. Urban Green.* **2017**, *23*, 44–53. [[CrossRef](#)]
32. Cabral, I.; Costa, S.; Weiland, U.; Bonn, A. Urban Gardens as Multifunctional Nature-Based Solutions for Societal Goals in a Changing Climate. In *Nature-Based Solutions to Climate Change Adaptation in Urban Areas*; Kabisch, N., Korn, H., Stadler, J., Bonn, A., Eds.; Springer International Publishing: Cham, Switzerland, 2017; pp. 237–253. ISBN 978-3-319-53750-4.

33. Senatsverwaltung für Umwelt, Verkehr und Klimaschutz. Daten und Fakten zu Kleingärten/Land Berlin. Available online: https://www.berlin.de/senuvk/umwelt/stadtgruen/kleingarten/de/daten_fakten/index.shtml (accessed on 31 May 2018).
34. Senatsverwaltung für Stadtentwicklung und Umwelt. Das bunte Grün. Kleingärten in Berlin. 2012. Available online: <https://www.berlin.de/senuvk/umwelt/stadtgruen/kleingarten/downloads/Kleingartenbroschuere.pdf> (accessed on 31 May 2018).
35. Armstrong, D. A survey of community gardens in upstate New York: Implications for health promotion and community development. *Health Place* **2000**, *6*, 319–327. [[CrossRef](#)]
36. Edmondson, J.L.; Stott, I.; Davies, Z.G.; Gaston, K.J.; Leake, J.R. Soil surface temperatures reveal moderation of the urban heat island effect by trees and shrubs. *Sci. Rep.* **2016**, *6*, 33708. [[CrossRef](#)]
37. Borysiak, J.; Mizgajski, A.; Speak, A. Floral biodiversity of allotment gardens and its contribution to urban green infrastructure. *Urban Ecosyst.* **2017**, *20*, 323–335. [[CrossRef](#)]
38. Tresch, S.; Frey, D.; Bayon, R.-C.L.; Zanetta, A.; Rasche, F.; Fliessbach, A.; Moretti, M. Litter decomposition driven by soil fauna, plant diversity and soil management in urban gardens. *Sci. Total Environ.* **2019**, *658*, 1614–1629. [[CrossRef](#)]
39. Speak, A.F.; Mizgajski, A.; Borysiak, J. Allotment gardens and parks: Provision of ecosystem services with an emphasis on biodiversity. *Urban For. Urban Green.* **2015**, *14*, 772–781. [[CrossRef](#)]
40. Langemeyer, J.; Latkowska, M.J.; Gómez-Baggethun, E.N.; Voigt, A.; Calvet-Mir, L.; Pourias, J.; Camps-Calvet, M.; Orsini, F.; Breuste, J.; Artmann, M.; et al. Ecosystem services from urban gardens. In *Urban Allotment Gardens in Europe*; Bell, S., Fox-Kämper, R., Keshavarz, N., Benson, M., Caputo, S., Noori, S., Voigt, A., Eds.; Routledge: London, UK; New York, NY, USA, 2018; pp. 115–141. ISBN 978-1-138-92109-2.
41. Deutscher Bundestag. Bundeskleingartengesetz. BKleingG, Bundesgesetzblatt 2006. Available online: <http://www.gesetze-im-internet.de/bkleingg/BKleingG.pdf> (accessed on 31 March 2020).
42. Norton, B.A.; Coutts, A.M.; Livesley, S.J.; Harris, R.J.; Hunter, A.M.; Williams, N.S.G. Planning for cooler cities: A framework to prioritise green infrastructure to mitigate high temperatures in urban landscapes. *Landsc. Urban Plan.* **2015**, *134*, 127–138. [[CrossRef](#)]
43. Schlegelmilch, A. The Cooling Potential of Allotment Gardens during Summer—Case Study “Kleingartenkolonie Johannisberg” in Berlin. Master’s Thesis, Technische Universität Berlin, Berlin, Germany, 2018.
44. Amt für Statistik Berlin Brandenburg. Einwohnerwachstum in Berlin setzt sich 2018 fort—Jedoch mit nachlassender Dynamik. 2018. Available online: <https://www.statistik-berlin-brandenburg.de/pms/2018/18-10-02.pdf> (accessed on 31 March 2020).
45. Endlicher, W.; Lanfner, N. Meso- and Micro-Climatic Aspects of Berlin’s Urban Climate. *Die Erde* **2003**, *3*, 277–293.
46. Kottek, M.; Grieser, J.; Beck, C.; Rudolf, B.; Rubel, F. World Map of the Köppen-Geiger climate classification updated. *Meteorol. Z.* **2006**, *15*, 259–263. [[CrossRef](#)]
47. Amt für Statistik Berlin-Brandenburg. Kleine Berlin-Statistik. 2019. Available online: https://www.statistik-berlin-brandenburg.de/produkte/kleinstatistik/AP_KleineStatistik_DE_2019_BE.pdf (accessed on 31 March 2020).
48. Senatsverwaltung für Stadtentwicklung und Wohnen. Umweltatlas. Available online: <https://www.stadtentwicklung.berlin.de/umwelt/umweltatlas/> (accessed on 24 March 2019).
49. Schubert, S.; Grossman-Clarke, S. The Influence of green areas and roof albedos on air temperatures during Extreme Heat Events in Berlin, Germany. *Meteorol. Z.* **2013**, *22*, 131–143. [[CrossRef](#)]
50. Senatsverwaltung für Stadtentwicklung und Wohnen. Umweltatlas Berlin/Städtebauliche Dichte-GFZ/GRZ. 2016. Available online: https://fbinter.stadt-berlin.de/fb/index.jsp?loginkey=showMap&mapId=wmsk01_02versieg2016@senstadt (accessed on 31 March 2020).
51. Senatsverwaltung für Stadtentwicklung und Wohnen. Umweltatlas Berlin/Flächennutzung, Stadtstruktur 2015 und Versiegelung. 2016. Available online: https://fbinter.stadt-berlin.de/fb/index.jsp?loginkey=showMap&mapId=wmsk01_02versieg2016@senstadt (accessed on 31 March 2020).
52. Lindberg, F.; Holmer, B.; Thorsson, S. SOLWEIG 1.0—Modelling spatial variations of 3D radiant fluxes and mean radiant temperature in complex urban settings. *Int. J. Biometeorol.* **2008**, *52*, 697–713. [[CrossRef](#)]

53. Rost, A.T.; Liste, V.; Seidel, C.; Matscherroth, L. Temperature and Humidity Measurements in Allotment Gardens in Berlin 2018 and Supplementary Temperature Data of Urban and Rural Measurement Stations of TU Berlin. 2020. Available online: <https://depositor.tu-berlin.de/handle/11303/10989.2> (accessed on 31 March 2020).
54. Fenner, D.; Holtmann, A.; Meier, F.; Langer, I.; Scherer, D. Contrasting changes of urban heat island intensity during hot weather episodes. *Environ. Res. Lett.* **2019**, *14*, 124013. [[CrossRef](#)]
55. DWD Climate Data Center. *Historical Hourly Station Observations of 2m Air Temperature and Humidity for Germany*, version 006; DWD Climate Data Center: Offenbach am Main, Germany, 2018.
56. Fenner, D.; Meier, F.; Scherer, D.; Polze, A. Spatial and temporal air temperature variability in Berlin, Germany, during the years 2001–2010. *Urban Clim.* **2014**, *10*, 308–331. [[CrossRef](#)]
57. Erell, E.; Williamson, T. Intra-urban differences in canopy layer air temperature at a mid-latitude city. *Int. J. Clim.* **2007**, *27*, 1243–1255. [[CrossRef](#)]
58. Middel, A.; Häb, K.; Brazel, A.J.; Martin, C.A.; Guhathakurta, S. Impact of urban form and design on mid-afternoon microclimate in Phoenix Local Climate Zones. *Landsc. Urban Plan.* **2014**, *122*, 16–28. [[CrossRef](#)]
59. Quanz, J.A.; Ulrich, S.; Fenner, D.; Holtmann, A.; Eimermacher, J. Micro-Scale Variability of Air Temperature within a Local Climate Zone in Berlin, Germany, during Summer. *Climate* **2018**, *6*, 5. [[CrossRef](#)]
60. DWD Climate Data Center. *Historical Daily Station Observations (Temperature, Pressure, Precipitation, Sunshine Duration, etc.) for Germany*, version v006; DWD Climate Data Center: Offenbach am Main, Germany, 2018.
61. Kruskal, W.H.; Wallis, W.A. Use of Ranks in One-Criterion Variance Analysis. *J. Am. Stat. Assoc.* **1952**, *47*, 583–621. [[CrossRef](#)]
62. Dunn, O.J. Multiple Comparisons Using Rank Sums. *Technometrics* **1964**, *6*, 241–252. [[CrossRef](#)]
63. Benjamini, Y.; Hochberg, Y. Controlling the False Discovery Rate: A Practical and Powerful Approach to Multiple Testing. *J. R. Stat. Soc. B* **1995**, *57*, 289–300. [[CrossRef](#)]
64. Wilks, D.S. *Statistical Methods in Atmospheric Sciences*, 2nd ed.; Academic Press: Burlington, MA, USA, 2005; ISBN 978-0-12-751966-1.
65. Unger, J. Intra-urban relationship between surface geometry and urban heat island: Review and new approach. *Clim. Res.* **2004**, *27*, 253–264. [[CrossRef](#)]
66. Potchter, O.; Cohen, P.; Bitan, A. Climatic behavior of various urban parks during hot and humid summer in the mediterranean city of Tel Aviv, Israel. *Int. J. Clim.* **2006**, *26*, 1695–1711. [[CrossRef](#)]
67. Chow, W.T.L.; Pope, R.L.; Martin, C.A.; Brazel, A.J. Observing and modeling the nocturnal park cool island of an arid city: Horizontal and vertical impacts. *Theor. Appl. Clim.* **2011**, *103*, 197–211. [[CrossRef](#)]
68. Ronda, R.J.; Steeneveld, G.J.; Heusinkveld, B.G.; Attema, J.J.; Holtslag, A.A.M. Urban Finescale Forecasting Reveals Weather Conditions with Unprecedented Detail. *Bull. Am. Meteorol. Soc.* **2017**, *98*, 2675–2688. [[CrossRef](#)]
69. Maronga, B.; Gross, G.; Raasch, S.; Banzhaf, S.; Forkel, R.; Heldens, W.; Kanani-Sühring, F.; Matzarakis, A.; Mauder, M.; Pavlik, D.; et al. Development of a new urban climate model based on the model PALM—Project overview, planned work, and first achievements. *Meteorol. Z.* **2019**, *28*, 105–119. [[CrossRef](#)]
70. Maronga, B.; Banzhaf, S.; Burmeister, C.; Esch, T.; Forkel, R.; Fröhlich, D.; Fuka, V.; Gehrke, K.F.; Geletič, J.; Giersch, S.; et al. Overview of the PALM model system 6.0. *Geosci. Model Dev.* **2020**, *13*, 1335–1372. [[CrossRef](#)]
71. Vieira, J.; Matos, P.; Mexia, T.; Silva, P.; Lopes, N.; Freitas, C.; Correia, O.; Santos-Reis, M.; Branquinho, C.; Pinho, P. Green spaces are not all the same for the provision of air purification and climate regulation services: The case of urban parks. *Environ. Res.* **2018**, *160*, 306–313. [[CrossRef](#)]
72. Weng, Q.; Liu, H.; Lu, D. Assessing the effects of land use and land cover patterns on thermal conditions using landscape metrics in city of Indianapolis, United States. *Urban Ecosyst.* **2007**, *10*, 203–219. [[CrossRef](#)]
73. Schwarz, N.; Schlink, U.; Franck, U.; Grossmann, K. Relationship of land surface and air temperatures and its implications for quantifying urban heat island indicators: An application for the city of Leipzig (Germany). *Ecol. Indic.* **2012**, *18*, 693–704. [[CrossRef](#)]
74. Oke, T.R. City size and the urban heat island. *Atmos. Environ.* **1973**, *7*, 769–779. [[CrossRef](#)]
75. Huang, L.; Li, J.; Zhao, D.; Zhu, J. A fieldwork study on the diurnal changes of urban microclimate in four types of ground cover and urban heat island of Nanjing, China. *Build. Environ.* **2008**, *43*, 7–17. [[CrossRef](#)]
76. Tsilini, V.; Papantoniou, S.; Kolokotsa, D.-D.; Maria, E.-A. Urban gardens as a solution to energy poverty and urban heat island. *Sustain. Cities Soc.* **2015**, *14*, 323–333. [[CrossRef](#)]

77. Heusinkveld, B.G.; Steeneveld, G.J.; van Hove, L.W.A.; Jacobs, C.M.J.; Holtslag, A.A.M. Spatial variability of the Rotterdam urban heat island as influenced by urban land use. *J. Geophys. Res. Atmos.* **2014**, *119*, 677–692. [[CrossRef](#)]
78. European Commission. *Commission Staff Working Document. Guidance on a Strategic Framework for Further Supporting the Deployment of EU-Level Green and Blue Infrastructure*; European Commission: Brussels, Belgium, 2019.



© 2020 by the authors. Licensee MDPI, Basel, Switzerland. This article is an open access article distributed under the terms and conditions of the Creative Commons Attribution (CC BY) license (<http://creativecommons.org/licenses/by/4.0/>).